Report: Work done in the last 12 months

Partner: C3M

Prepared by: **Igor Grešovnik**

Project: **ENLUB**
Development of New Environmentally Acceptable Lubricants, Tribological Tests and Models for European Sheet Forming Industry
Contract Number G1RD-CT-2002-00740

Issued: **April 26, 2006**

1 Software environment for optimization and identification of model parameters

C3M was in charge for numerical modeling and identification of parameters for numerical models. For this purpose, the group is developing a software environment that enables efficient incorporation of new material models, analytical sensitivity analysis and optimisation. By this system, finite elements formulations and material laws are defined at symbolic level. The element stiffnesses, loads and corresponding element sensitivity routines are then generated by the symbolic mechanics system, which also generates the routines that can be readily incorporated in the global finite element environment.

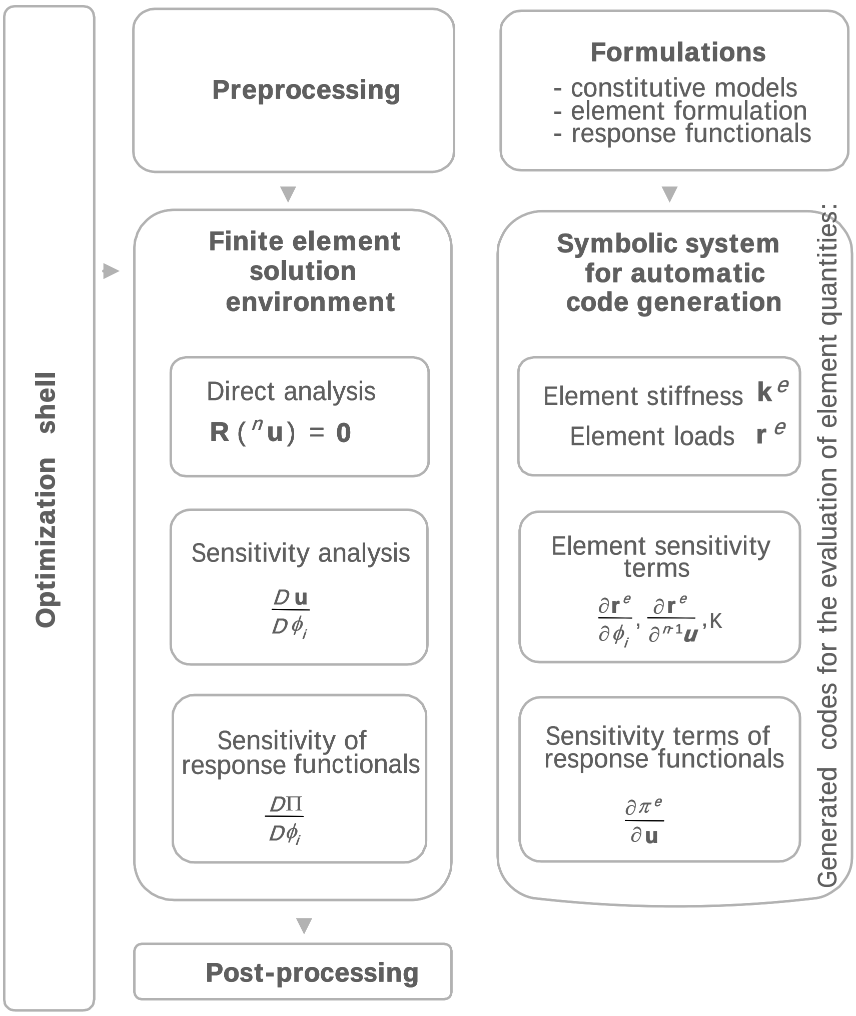

Figure 1: Scheme of the software environment for numerical modeling and optimisation.

After the complete direct problem is set up in the above environment for the finite element analysis, the numerical analysis can be connected with the optimization program *Inverse* in order to perform parametric studies, inverse identification of material parameters or process optimisation. *Inverse* provides an extensive optimisation environment with many useful features for solving industrial optimisation problems:

Flexible user interface implemented as a file interpreter o expression evaluator and file interpreter with nested command syntax enable flow control in a similar manner than do the high level programming languages. o high level commands enable simple use without necessity for flow control.
A collection of various optimization algorithms o The powerful *FSQP* algorithm is the basic optimization engine of the shell. o Unconstrained minimization of non-linear functions o Constraint minimization: variable bounds, linear and non-linear inequality and equality constraints
A collection of auxiliary tools o A palette of tabulating utilities for examining topology of the objective functions o Monte Carlo simulations for examination of nature of inverse solutions
Tools for parameterization of geometry o Spline interpolation functions
User defined variables for storing different types of data o Matrix, vector and scalar variables o Fields for storing discrete representations of continuum data (e.g. finite element meshes, scalar, vector & other fields)
Common operations on basic types of variables o Basic matrix and vector operations o Basic mathematical operations o Possibility of defining new operations
A general file interface for interfacing arbitrary simulation programs through files
Direct interface with simulation program ELFEN
Unlimited data transfer between different modules of the shell o All data is usable everywhere, results of one operation are accessible to following operations
Readily available reports about solution procedures o Output to terminal and to a file o All output except specially formatted data for further processing o Possibility of outputting virtually every information that exists in the shell
Different levels of use o Semi descriptive level o High level where some features of solution algorithm are controlled by the users o The highest level where also some basic algorithms are programmed by the user; in this case the shell can serve for providing a portion of algorithms, auxiliary utilities and utilities for interfacing system environment and simulation programme.
Openness o Easy adaptation for use with different simulation programmes o Possibility of using external modules for partial tasks (e.g. for interfacing the simulation programme)

Syntax checker and Debugger

- Syntax checker enables the user to discover syntax errors before running the projects which in many cases saves considerable amount of time.
- Debugger facilitates location of tricky errors which the user makes at the construction of solution procedure. It enables step-by-step execution of the solution procedure. The user can on-line monitor values of all shell variables, assign different values to them and executes additional shell commands.

Within the described period, the program was supplemented by the features that enable running optimisation from symbolic system Mathematica and exchange of data with this system. In this way, the optimization environment is directly connected to the finite element environment shown in Figure 1, which was necessary for better link between model development and application.

2 *Simulation and inverse analysis* of the strip reduction test

The strip reduction test was simulated (Figure 1), with sensitivity analysis of the simulated measurements (temperatures inside the groove and the drawing force) with respect to friction and heat transfer parameters performed.

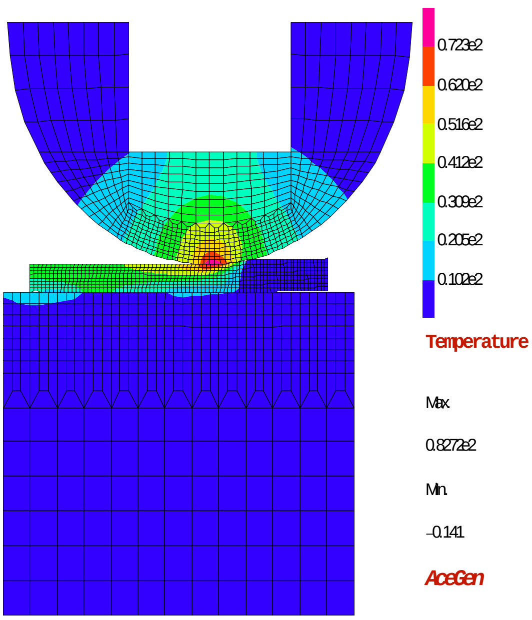

Figure 2: Finite element simulation of the strip reduction test: temperature field.

The following objective (discrepacy) function to be minimised has been defined for identification of the contact parameters:

$$f(\mathbf{p}) = \sum_{i=1}^{n} \int_{t_{\min}}^{t_{\max}} \left(T_i(t) - T_i^{(m)}\right)^2 \; dt + k_F \int_{t_{\min}}^{t_{\max}} \left(F(t) - F^{(m)}\right)^2 dt \quad , \tag{1}$$

where $T_i^{(m)}(t)$ is the course of the measured temperature at the sensor location *i*, $T_i(t)$ is the corresponding simulated temperature, $F^{(m)}(t)$ and $F(t)$ are the measured and simulated drawing forces, respectively, and time integration was replaced by appropriate sums within the FEM incrementation scheme. Corresponding parameter sensitivities are then expressed as

$$\frac{d\,f}{d\,p_k} = \sum_{i=1}^{nsens} \int_{t_{\min}}^{t_{\max}} 2\left(T_i\;(t) - T_i^{(m)}\right) \frac{d\,T_i\;(t)}{d\,p_k} d\,t + \int_{t_{\min}}^{t_{\max}} 2\left(F\;(t) - F^{(m)}\right) \frac{d\,F\;(t)}{d\,p_k} d\,t \;, \tag{2}$$

where the sensitivities of simulated temperatures at sensor locations and the drawing force were computed within the above mentioned analytical direct differentiation scheme.

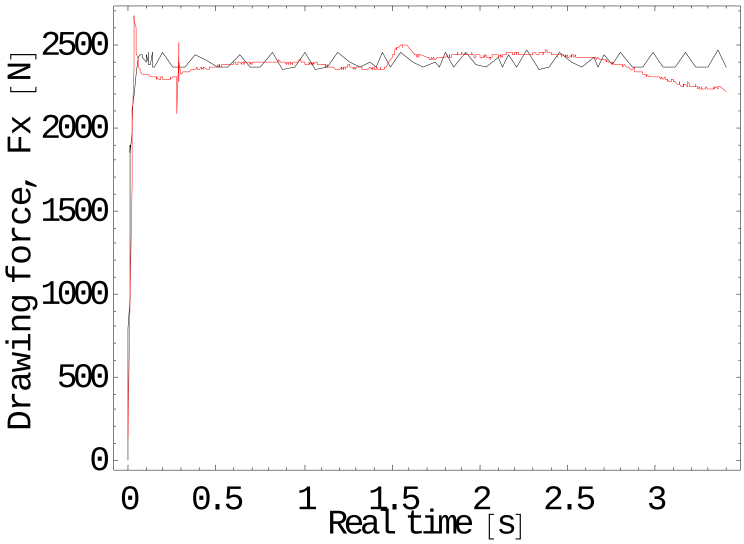

a)

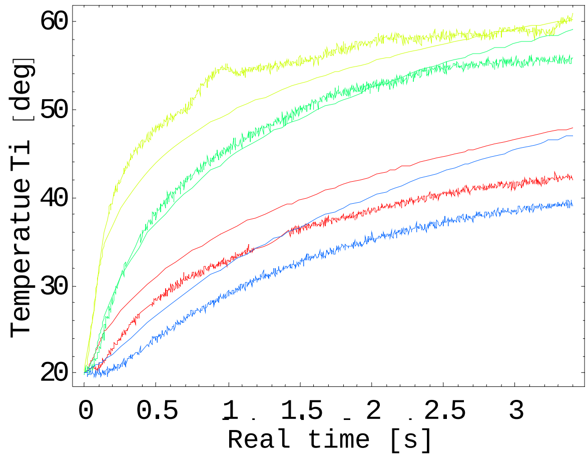

b)

Figure 3: Comparison of the simulated and measured drawing force (a) and temperatures at sensor locations (b).

Figure 3 shows simulated measurements compared to actual measurement data obtained at laboratory testing. Sensitivities of the simulated temperatures and the drawing force obtained by the direct differentiation method were used for calculation of derivatives of the objective function defined in equation (1).

Some sensitivities and direct terms that contribute to the temperature sensitivity part in equation (2) are shown below.

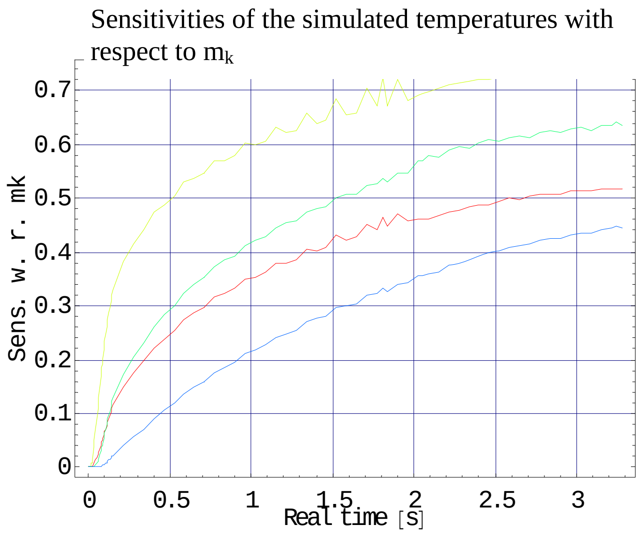

Sensitivities of the simulated temperatures with respect to h_{loc}

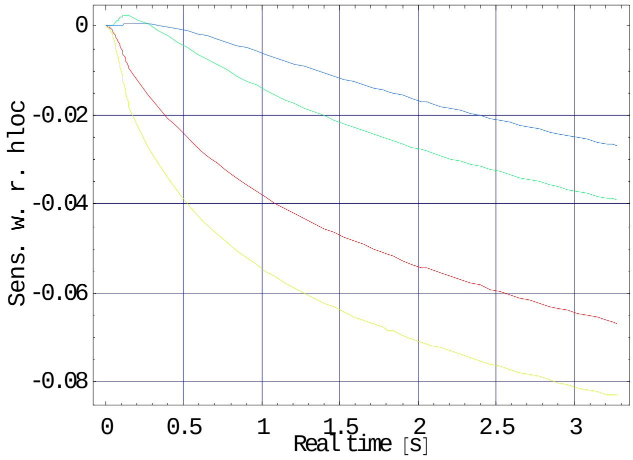

Difference between simulated and measured temperatures

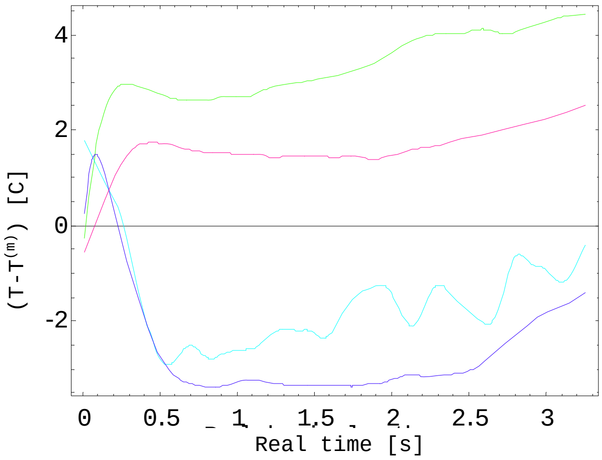

Squared difference between simulated and measured temperatures

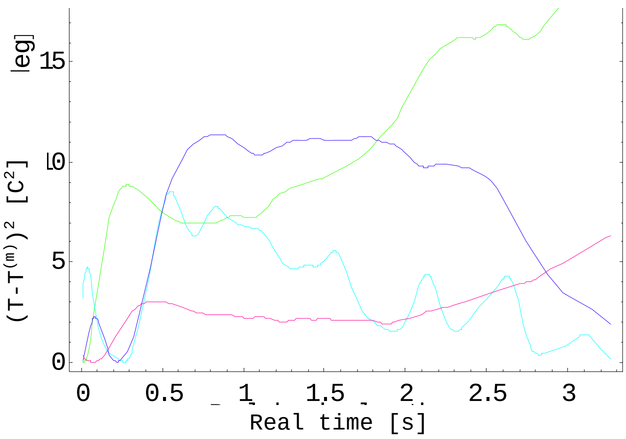

Sensitivities of the simulated temperatures with respect to m_k

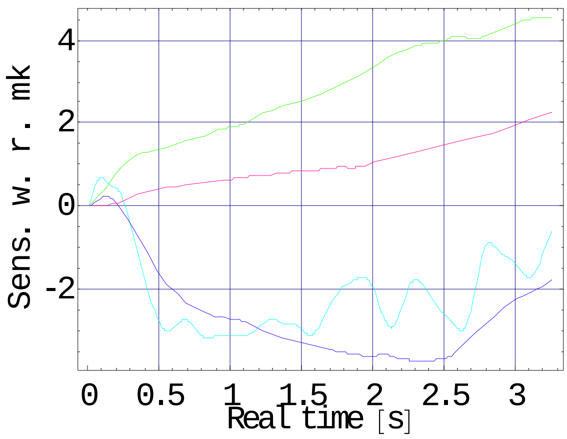

Sensitivities of the simulated temperatures with respect to h_{loc}

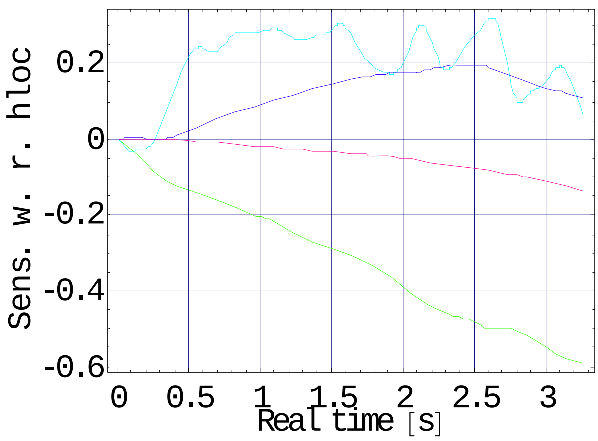

Figure 4: Contributions to the integrand of the temperature part in equation (2).

2.1 Indication of numerical noise and smoothing of response

Because of the noise in the temperature and force measurements and due to the discrete time integration scheme, we could expect that the objective function defined as above would also contain some level of noise. This was anlaysed by tabulating the response along varying parameters and along chosen directions in the parameter space. In this way the validity of the parameters calculated by minimization of the objective function could also be verified by tabulating along the lines passing through the obtained minima.

Sample studies are shown in Figure 5. Studies indicated that the level of noise contained in the response is substantial, and indicated how the optimization algorithm can be trapped in spurious minima generated by numerical noise (see e.g. Figure 5 b)). In some studies the temperature and force contributions to the objective function (eq. (1)) were separated in order to indicate which part is more noisy and more decisive for identification of individual parameters.

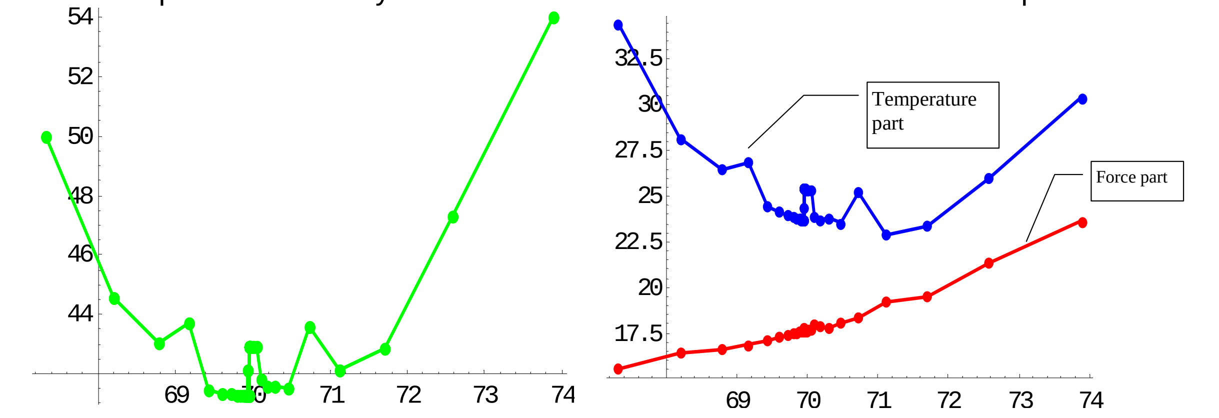

a) Variation of parameter 1

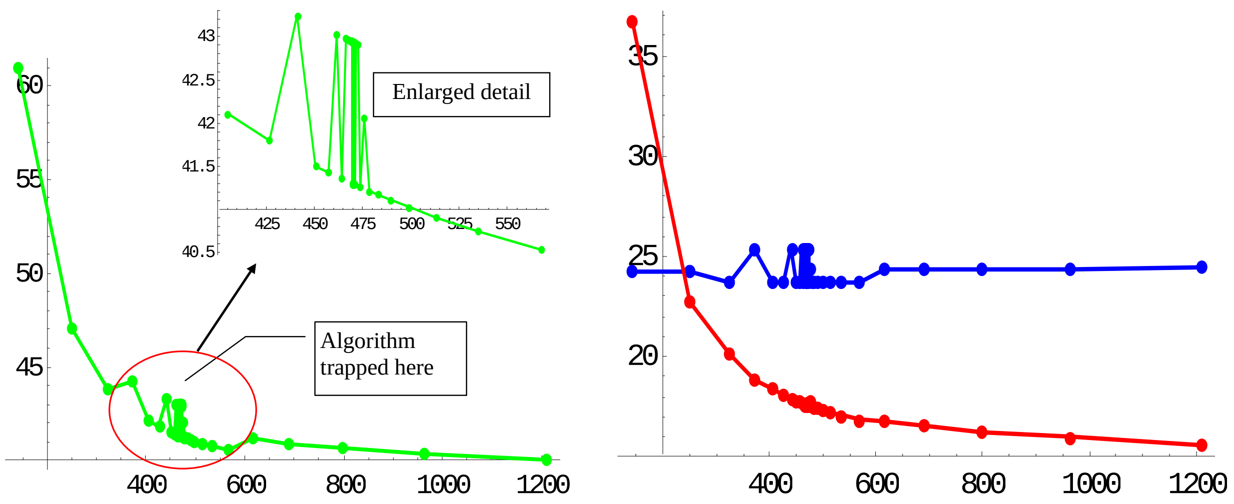

b) Variation of parameter 2

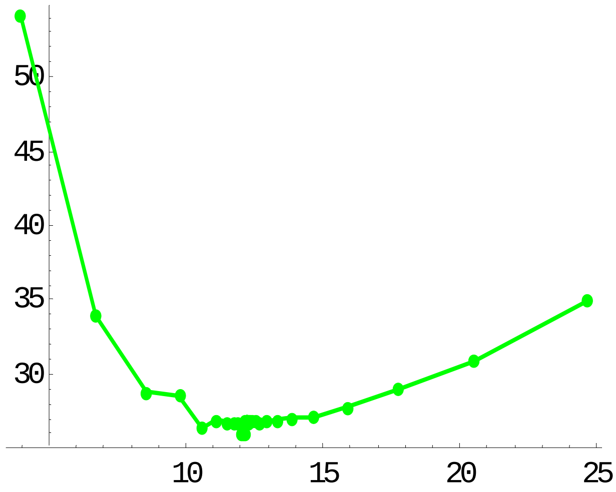

c) Variation of parameter 3

Figure 5: Parametric studies – sampling of the objective function against individual parameters.

An attempt has been made to improve the response properties (regarding algorithm performance) by smoothing the measured and simulated temperatures and forces. The data available at discrete times were replaced by continuous approximation. The moving least squares (MLS) approximation has been applied; cf. [2]. This kind of approximation was found very suitable for this purpose because it can adapt to variation of function values over an arbitrarily large parameter range (as opposed to ordinary least squares, which can provide good approximation only locally), and locally exhibits the properties of moving least squares approximation that efficiently level out the high frequency oscillations that are the consequence of numerical and measurement noise. Figure 6 shows the effect of MLS approximation used for obtaining continuous representation of measured forces without the typical high frequency oscillations.

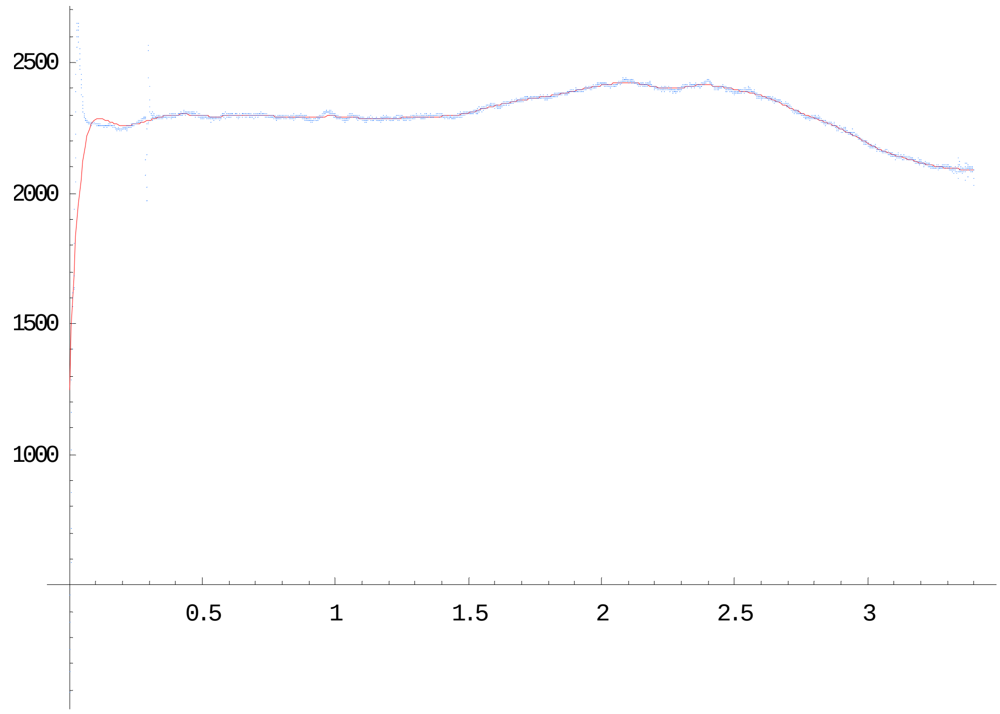

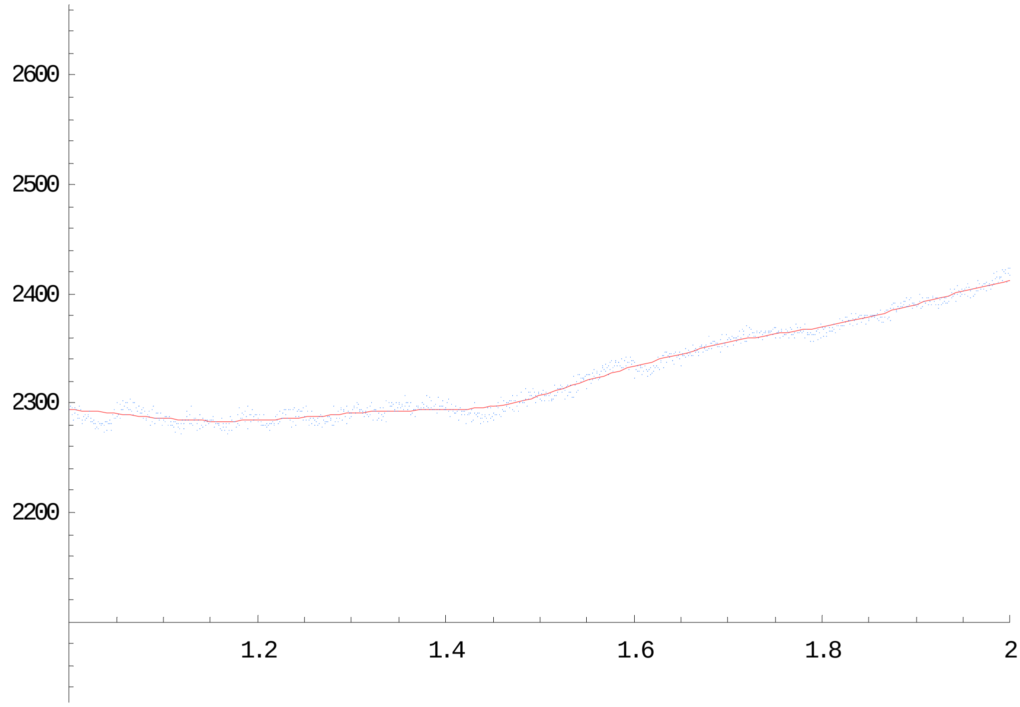

a) Smoothed force measurements. Blue points represent the measured samples and red curve the smooth approximation. Lower picture represents an enlarged detail.

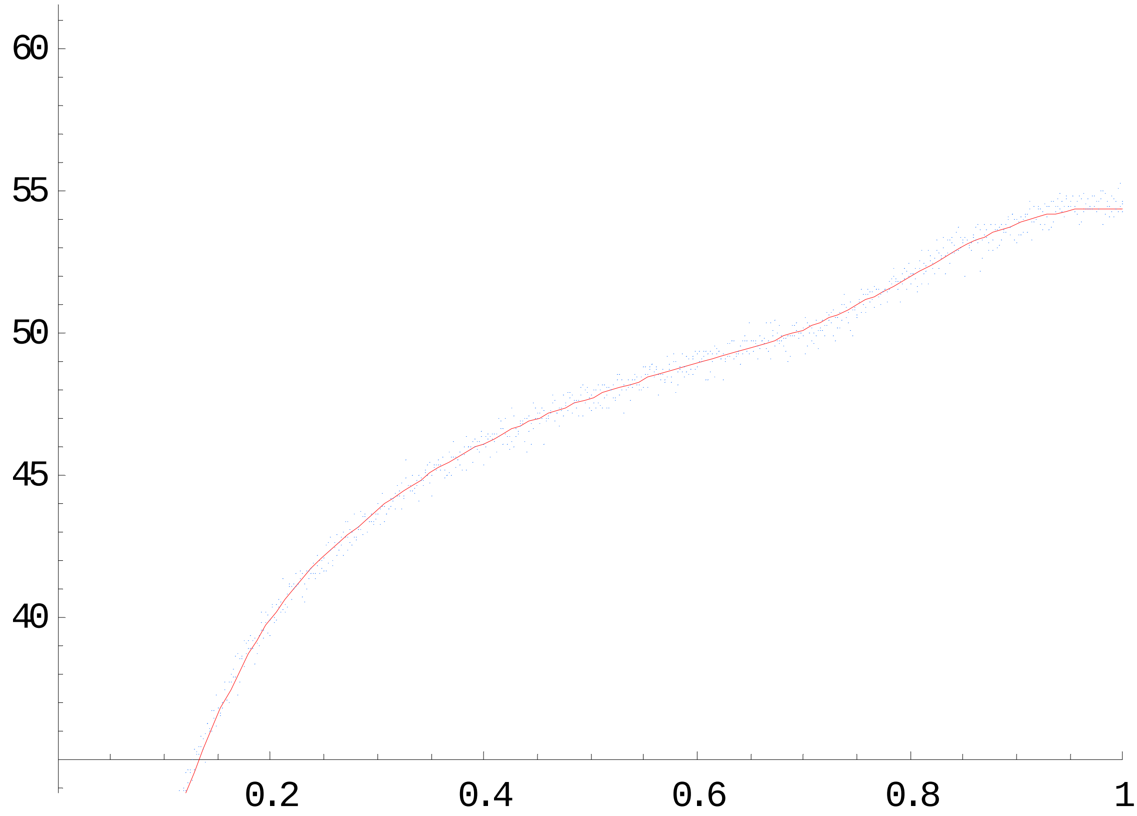

b) Approximation of measured temperature in the sensor No. 2 – enlarged detail.

Figure 6: Application of moving least squares approximation as a tool for smoothing the measurements.

The definition of the objective and function was updated by replacing the measured and simulated quantities in equation (1) by their continuous MLS approximation. The effect of this on smoothness of the response was observed by sampling the response along individual parameters in the same points as this was done for the originally defined objective function. Some results are shown in Figure 7. Comparison with Figure 5 shows that some improvement regarding smoothness of the response was achieved. However, the improvement was not sufficient to avoid the possibility that the minimization algorithm is trapped in spurious minima, which was also confirmed by trial runs of the algorithm with re-defined response functions using different starting values of parameters.

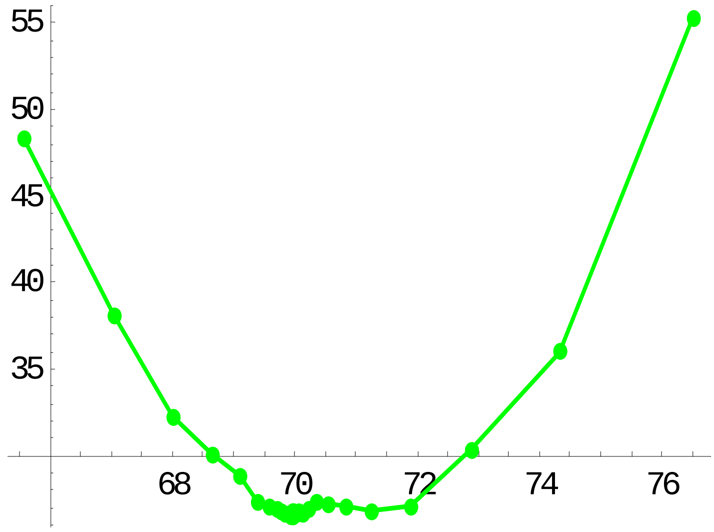

a) Variation of parameter 1

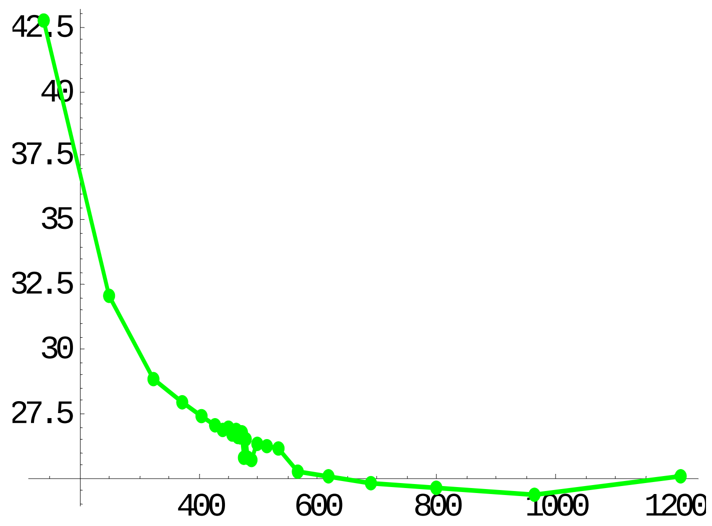

b) Variation of parameter 2

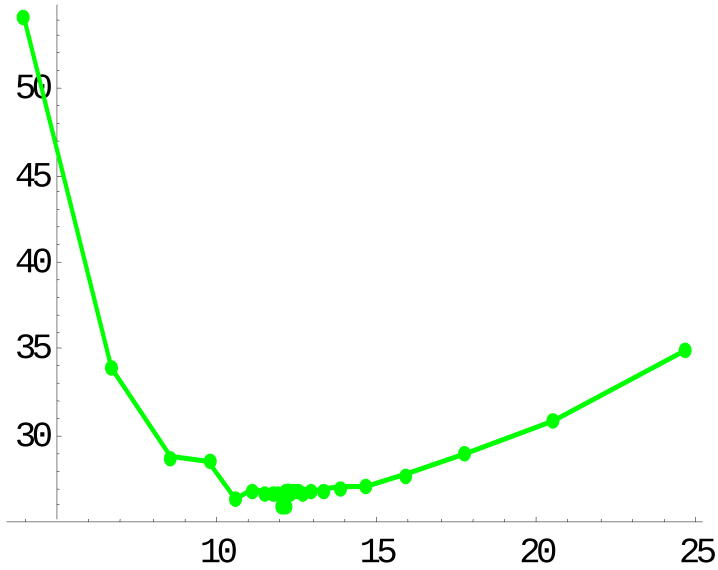

c) Variation of parameter 2

Figure 7: Variation of the objective function calculated by smoothed measurements and simulated measurements, along individual parameters.

2.2 Fixed time incrementation

It has been considered that changes of time increment scheme of the finite analysis could be one of the important sources of numerical noise. In adaptive increment adjustment, the length of time increments can change discontinuously when perturbing optimization parameters. In an attempt to further reduce the noise, the time incrementation scheme of the FEM analysis was constrained by switching off adaptive time step adjustment and using fixed increments instead. It turned that this significantly improved the smoothness of the objective function with respect to identified contact parameters, which can be seen in parametric studies shown in Figure 8. However, even with this approach the numerical noise is not eliminated to a level which would ensure reliable identification of parameters by the BFGS algorithm. Therefore, the algorithm was run from different starting points and the result with the lowest value of the objective function was considered for actual values of contact parameters.

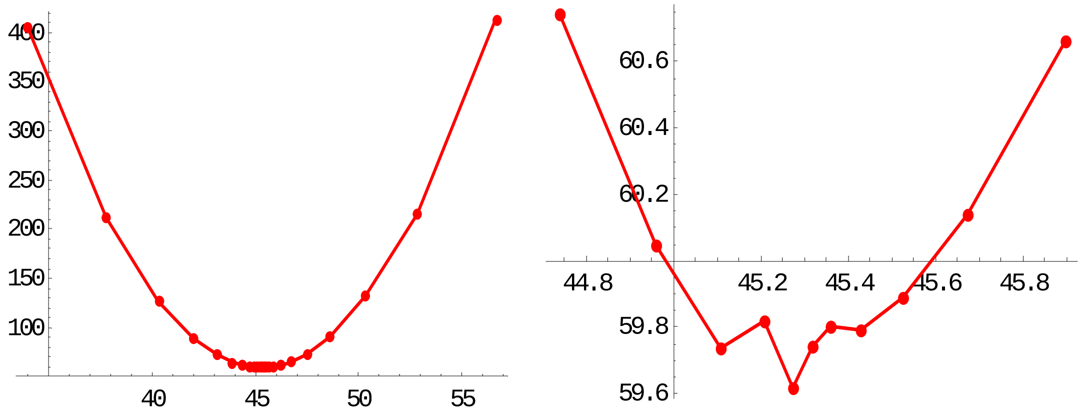

a) Variation of the objective function with respect to parameter 1, with enlarged detail around the directional minimum shown on the right-hand side.

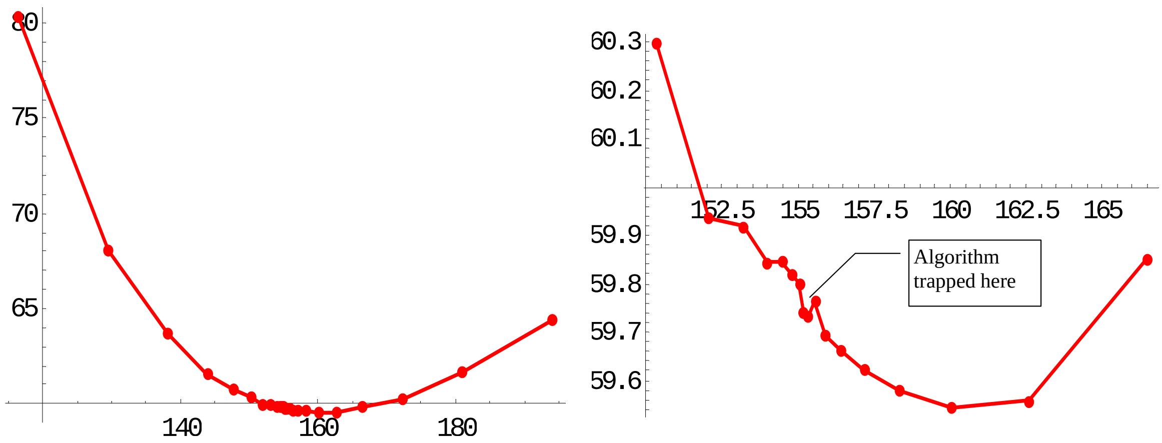

a) Variation of the objective function with respect to parameter 1, with enlarged detail around the value considered as optimal by the minimization algorithm.

Figure 8: Variation of the objective function calculated by smoothed measurements and simulated measurements, along individual parameters.

2.3 Optimization with approximated response

In order to overcome the difficulties related to numerical noise, another approach was applied at which optimisation was performed on a smooth approximated response. The objective function was first sampled in a number of randomly distributed points around the expected optimal parameters. The moving least squares approximation of the objective function was then generated on the basis of the sampled values, and this approximation was minimized. Since the approximation is smooth, minimisation by the BFGS algorithm is performed very efficiently and the algorithm does not experience any problems with trapping in fictive minima, i.e. the same results (in the scope of the specified tolerance) are obtained when running the algorithm from different starting points. After the first run, objective function was sampled in some additional points around the obtained minimum in order to refine the resolution of the MLS approximation in this area, and the algorithm was performed again on the improved approximation.

Since the objective function has been evaluated in a number of points when tabulating the response, these samples could be used for generation of the MLS approximation. This makes the number of samples much greater than it would be necessary for reliable identification of optimal parameters, but makes possibility of relatively accurate approximation and visualization of the response over a large domain (Figure 9, Figure 10). Two optima obtained with minimisation of performed directly on simulated response and the minimum of approximation are indicated in Figure 9. Around the first minimum, a number of regular patterns can be distinguished that were produced by tabulating the response along specified directions or for two dimensional tables.

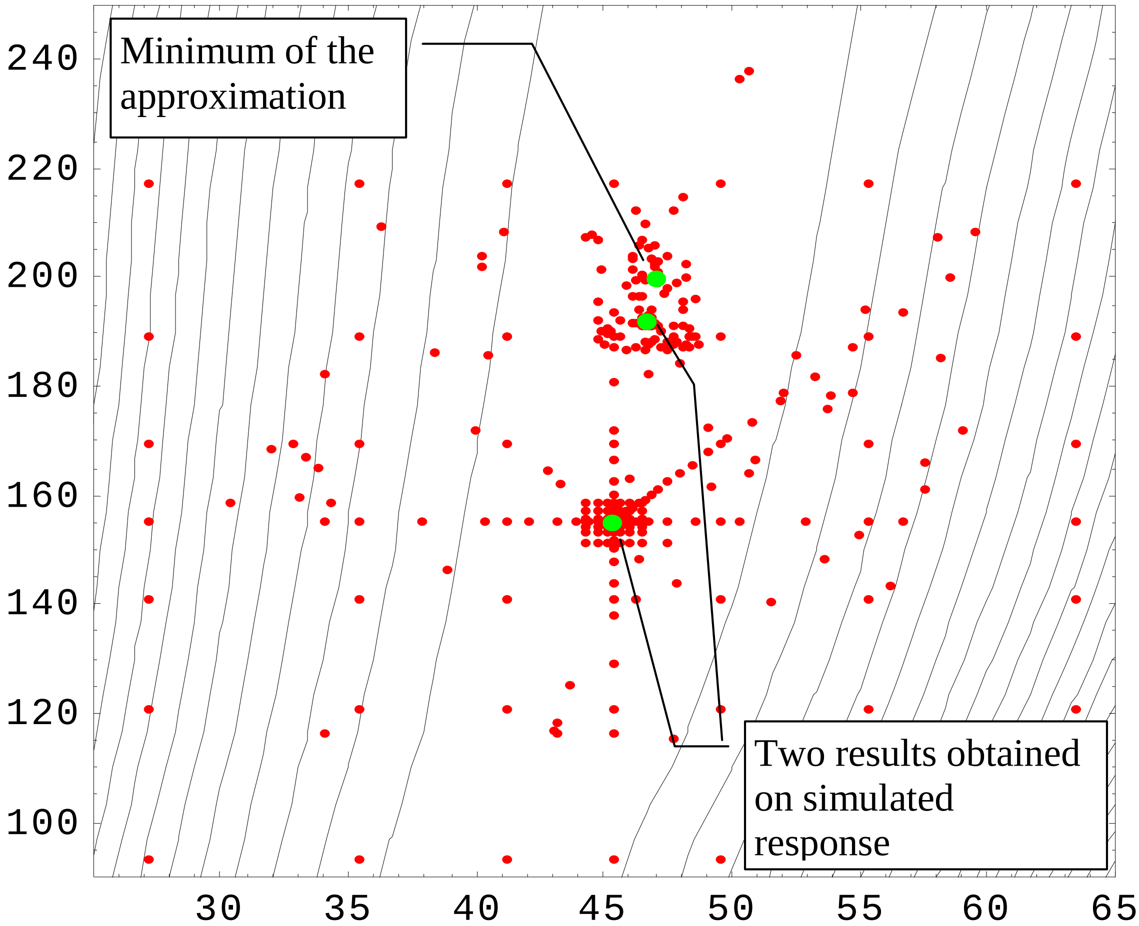

Figure 9: Contours of the approximated objective function with all the samples used for approximation.

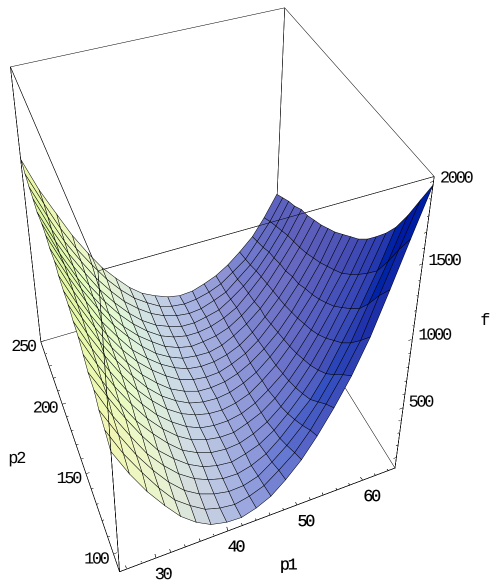

Figure 10: A 3D view of the approximated objective function based on the available samples.

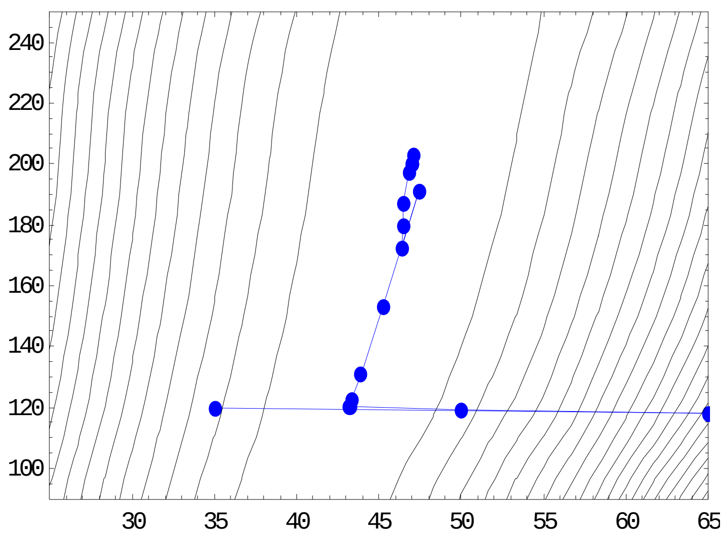

Figure 11: Optimisation path of the BFGS method applied to the MLS approximation of the objective function.

3 Application of results of inverse tests

The contact parameters obtained by the inverse analysis of the strip reduction tests were used in the numerical analysis of an industrial progressive forming process (Figure 12). Mechanisms of tool damage evolution have been studied by numerical analysis of the tool at microscopic level with boundary conditions obtained from the macroscopic analysis of the tool-workpiece contact interface (Figure 13).

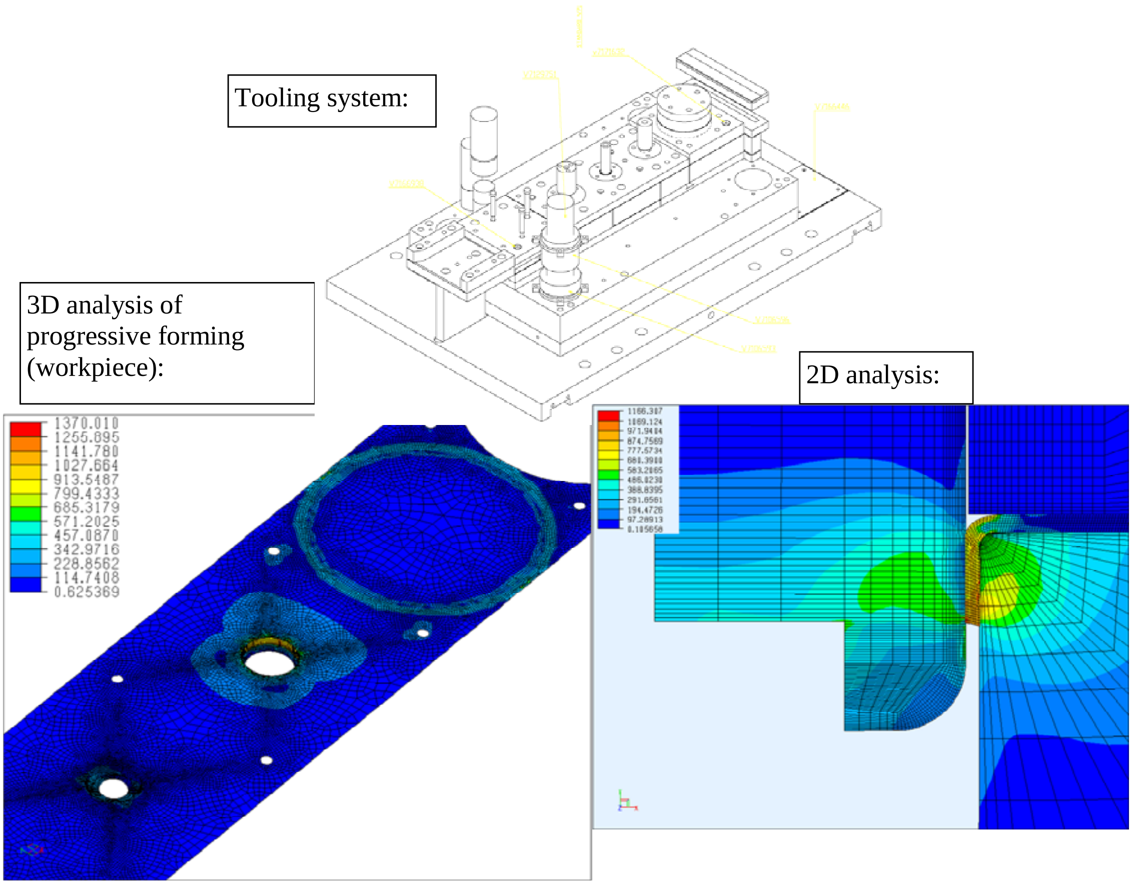

Figure 12: Progressive forming simulation: tooling set-up and workpiece.

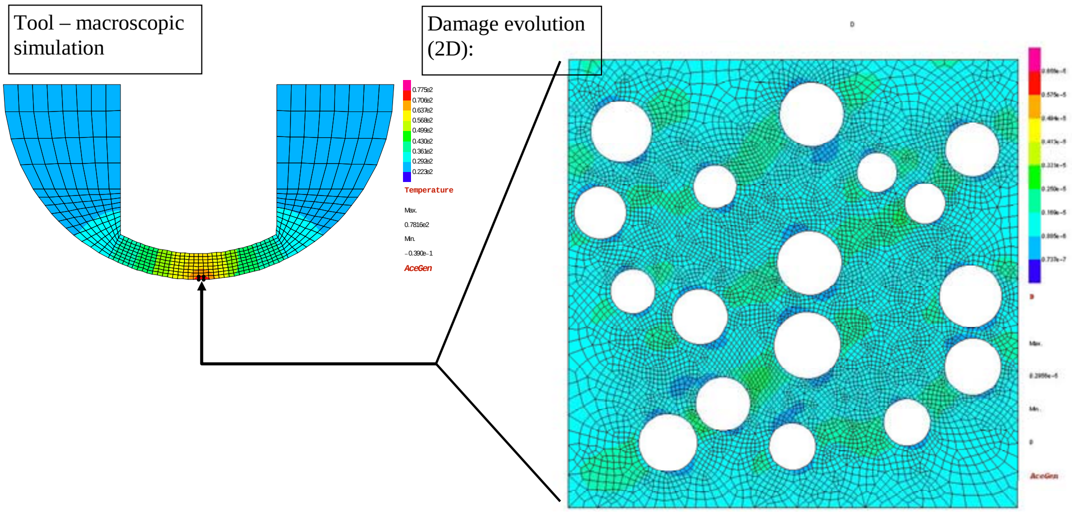

Figure 13: Study of tool damage evolution next to the tool-workpiece interface.

References:

[1] P. Michaleris, D. A. Tortorelli, C. A Vidal, *Tangent Operators and Design Sensitivity Formulations for Transient Non-Linear Coupled Problems with Applications to Elastoplasticity,* Int. Jour. For Numerical Methods in Engineering, vol. 37, pp. 2471-2499, John Wiley & Sons, 1994.

[2] P. Breitkopf, A. Rassineux, P. Villon, An Introduction to the Moving Least Squares Meshfree Methods, Revue Europenne des lments Finis, Volume 11 - No 7-8/2002.